

EPR of a $\langle 001 \rangle$ Si interstitial complex in irradiated silicon*

K. L. Brower

Sandia Laboratories, Albuquerque, New Mexico 87115

(Received 16 September 1975; revised manuscript received 8 December 1975)

This paper deals with an electron-paramagnetic-resonance study of the Si-B3 center, which was first reported by Daly. The Si-B3 center is a secondary defect which forms upon annealing between 50 and 175°C in irradiated boron-doped silicon and is stable up to $\approx 500^\circ\text{C}$. Our studies indicate that the Si-B3 center exhibits only a high-temperature stress response which is indicative of a thermally activated atomic reorientation at $T \gtrsim 400^\circ\text{C}$. This defect does not exhibit a low-temperature stress response indicative of Jahn-Teller effects; consequently, the Si-B3 center has inherent D_{2d} symmetry by virtue of its molecular structure. The kinetics of this defect, the nature of the ^{29}Si hyperfine interactions, and the symmetry of the defect suggest that the Si-B3 corresponds to either a $\langle 001 \rangle$ Si di-interstitial or a $\langle 001 \rangle$ Si split interstitial. The Si-B3 center appears to be similar but not identical to the Si-P6 center, which Lee and Corbett have recently suggested corresponds to a $\langle 001 \rangle$ Si di-interstitial.

I. INTRODUCTION

Several years ago Daly¹ found a new center which he labeled Si-B3. He characterized this defect in terms of its \bar{g} dyadic and the conditions under which it could be produced. The conditions which Daly picked were such that there was not sufficient intensity in the spectrum to detect any hyperfine structure which would further aid in its identification. Daly speculated that perhaps this center, which resembled the vacancy in its symmetry, might be a vacancy associated with some other defect, like an impurity interstitial located in a $\langle 001 \rangle$ direction.

During the course of our EPR studies on irradiated silicon, we encountered the same spectrum. We were especially intrigued by its symmetry properties which suggested that this defect might be a rather simple and fundamental type of center. Of the 40 or so paramagnetic defects reported so far in irradiated silicon,¹⁻⁵ only three other centers—the Si-G1,⁶ Si-A5,³ and Si-G25⁵—are known to have this symmetry. After measuring this spectrum as a function of impurity concentration, neutron fluence, and annealing temperature, we were able to optimize its intensity. Under optimum conditions the Si-B3 spectrum corresponds to one of the strongest EPR signals that we have observed in irradiated silicon. The results of our EPR studies on the Si-B3 center which are presented in this paper lead us to believe that the Si-B3 center is a $\langle 001 \rangle$ Si interstitial complex. In particular, this complex appears to correspond to either a $\langle 001 \rangle$ Si di-interstitial or a $\langle 001 \rangle$ Si split interstitial.

One other defect has been observed with EPR in irradiated silicon whose basic symmetry and structure appears to be generically related to the Si-B3 center. Some years ago Jung and Newell⁷

found a rather unusual defect (IX, more recently labeled Si-P6) in irradiated silicon which has D_2 symmetry at room temperature. Recently, Lee and Corbett⁸ have reexamined this defect and found that at lower temperatures this defect distorts to C_{1h} symmetry. They suggest that this defect is in essence a $\langle 001 \rangle$ Si di-interstitial. Although the Si-B3 and Si-P6 centers are distinct, they do appear to be similar.

Some of the properties of the Si-B3 center as observed by EPR resemble the properties associated with the defect responsible for internal friction peak IV found by Tan, Berry, and Frank.⁹ They have concluded from their internal-friction studies on boron-implanted silicon that peak IV is very likely a “neutral $\langle 001 \rangle$ silicon self-interstitial” (see Fig. 4 of Ref. 9).

II. EXPERIMENTAL RESULTS

A. Technique and samples

The measurements reported in this paper were made using a *K*-band superheterodyne EPR spectrometer. Spectra were taken with sample temperatures ranging from 15 to 50 K.

The samples which were used in this study were extracted from two different silicon ingots (214 and 226). The 214 samples came from an ingot of Lopex silicon doped with boron enriched with ^{10}B ($I=3$) to 95%; the resistivity of these *p*-type samples was 0.425 to 0.575 Ω cm. The 226 samples were extracted from an ingot of vacuum-float-zone silicon doped with 10^{15} B/cm³ and 10^{17} C/cm³. The carbon used to dope this ingot consisted of 60.1% ^{13}C and 39.9% ^{12}C . This was the same material as used in our EPR studies of the carbon interstitialcy¹⁰ (Si-G11).² These samples were especially useful in establishing the possible role of boron, oxygen, and carbon in the structure of

the Si-B3 center. We were unable to see the Si-B3 spectrum in neutron-irradiated crucible-grown Ga-doped silicon, Lopex Al-doped silicon, or crucible-grown B-doped silicon.

Natural oxygen is almost impossible to detect with EPR through the hyperfine interactions since the only isotope of oxygen with a nonzero nuclear spin (^{17}O , $I = \frac{5}{2}$) is only 0.037% naturally abundant. Infrared measurements made by Stein on our 214 samples failed to detect any oxygen, which means that the oxygen concentration is $< 10^{16}$ O/cm 3 .¹¹ We also checked for oxygen with EPR by measuring the intensity of the Si-SL1 center which has been identified as the neutral charge state of the vacancy-oxygen center.^{12,13} We have observed that this defect can be observed with EPR in electron, neutron, or ion-bombarded silicon independent of the position of the Fermi level.¹³ Using this defect as a monitor for oxygen, we observed in our 214 samples only a trace of the Si-SL1 spectrum corresponding to an oxygen concentration of $\approx 10^{15}$ O/cm 3 . Since we were able to see $\approx 5 \times 10^{16}$ Si-B3 centers/cm 3 in our 214 samples (Sec. II B), oxygen cannot be a part of the structure of the Si-B3 center.

There is no evidence which suggests that carbon is present in our 214 samples. In both electron- and neutron-irradiated 214 samples, we were unable to detect the Si-G11 spectrum, which has been identified as a carbon interstitialcy,¹⁰ even though we could see the positive divacancy (Si-G6).¹⁴ Although ^{13}C ($I = \frac{1}{2}$) is 1.108% naturally abundant, the ^{13}C hyperfine lines could be ob-

scured, if present, by the ^{29}Si hyperfine structure. Consequently, our studies were extended to the 226 samples which were doped with carbon enriched with ^{13}C . Under these conditions the role of carbon in the structure of the Si-B3 center should be apparent in the hyperfine structure of the Si-B3 spectrum (Secs. II C and III C).

In order to observe the Si-B3 spectrum the irradiated sample must be annealed at a temperature > 175 ,¹ but < 500 °C; the isochronal annealing behavior of the Si-B3 is shown in Fig. 1 (see also Ref. 1). This anneal accomplishes two things. First, it results in the formation of Si-B3 centers which are not present in the lattice damage following irradiation at ≈ 50 °C (Sec. II D). Second, this anneal also lowers the Fermi level into a region where the Si-B3 centers are paramagnetic. In this respect it was usually necessary to anneal our higher-fluence neutron-irradiated samples at higher temperatures (≈ 350 °C) in order to convert the defect from the diamagnetic to the paramagnetic charge state (Sec. II D).

B. Fluence dependence

The relative intensity of the Si-B3 spectrum as observed in our 214 samples as a function of neu-

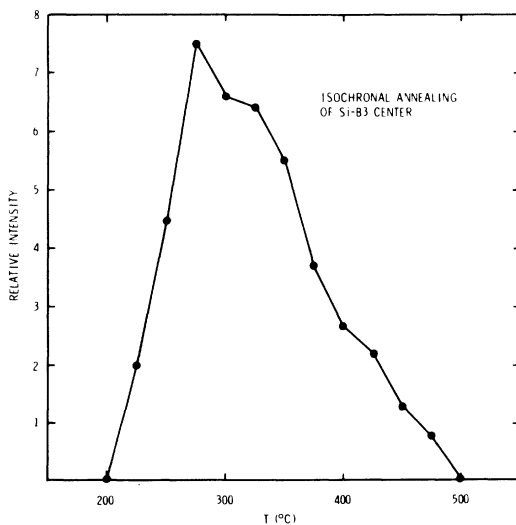


FIG. 1. Relative intensity of the Si-B3 center vs temperature at which 20-min isochronal anneals were performed. These measurements were obtained from sample 226-1 which had been neutron irradiated to a fluence of 3.12×10^{14} n/cm 2 .

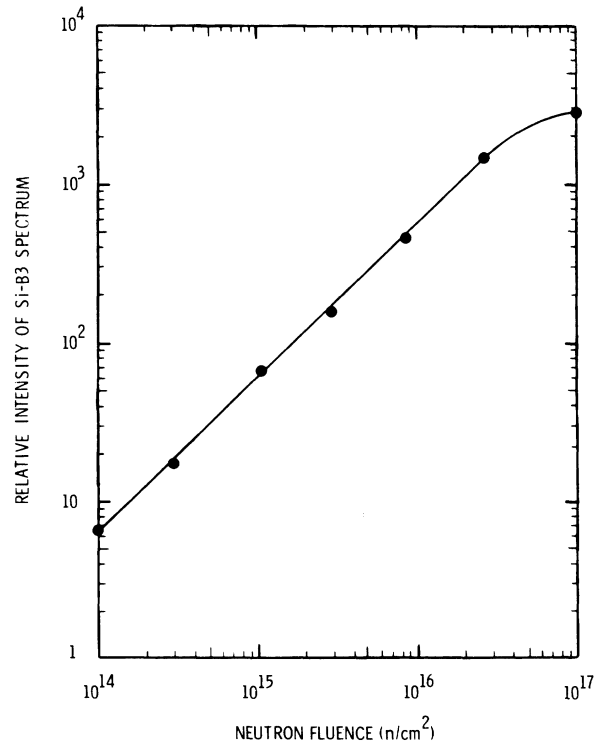


FIG. 2. Relative intensity of the Si-B3 center vs neutron fluence. The 214 samples used in these measurements were annealed at 350 °C for 20 min after irradiation.

tron fluence is shown in Fig. 2. The neutron irradiations were accomplished with the Sandia annular-core pulse reactor.¹⁵ During neutron irradiation, the temperature of our samples was $\approx 50^\circ\text{C}$. At 10^{17} n/cm^2 the intensity of the spectrum corresponds to $\approx 5 \times 10^{16} \text{ Si-B3 centers/cm}^3$;

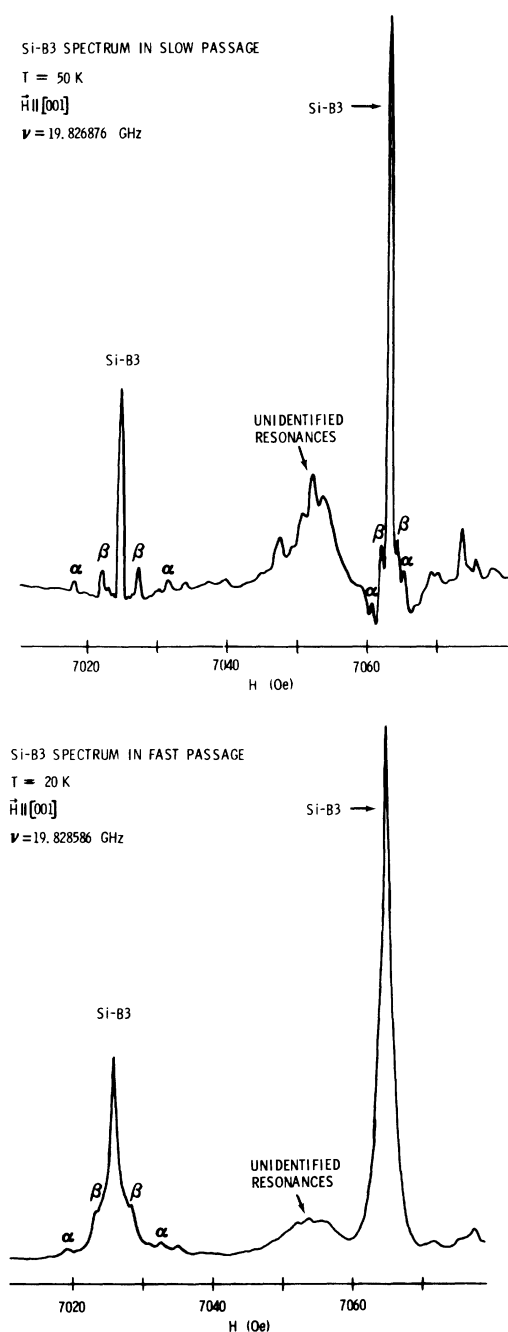


FIG. 3. Si-B3 EPR spectra. These spectra were observed with a *K*-band superheterodyne spectrometer from 214 samples annealed at 350°C for 20 min after an irradiation of 10^{17} n/cm^2 .

this is one of the strongest EPR signals we have observed in irradiated silicon. Its production rate in these samples is essentially linear with neutron fluence. The departure from linearity at 10^{17} n/cm^2 may reflect the depletion of boron. For example, if the Si-B3 center is an intrinsic defect, then it is paramagnetic in an odd charge state. In this case saturation of the Si-B3 spectrum would occur once the acceptors (boron) which compensate the positively charged Si-B3 centers are exhausted. At a fluence of $3 \times 10^{17} \text{ n/cm}^2$, the Si-B3 spectrum is not present after annealing at 350°C for 20 min. Apparently, the Fermi level is higher up in the band gap and all of the Si-B3 centers are diamagnetic.

C. Si-B3 spectrum

The Si-B3 spectrum as observed in our 214 samples and illustrated in Fig. 3 is characterized by a pair of Zeeman lines¹⁶ indicative of a defect having an electronic spin of $\frac{1}{2}$. The satellite structure labeled α and β in Fig. 3 arises from ^{29}Si hyperfine interactions; the ^{29}Si isotope has a nuclear spin of $\frac{1}{2}$ and is 4.70% naturally abundant. The intensity of the α ^{29}Si hyperfine lines relative to the Zeeman line clearly corresponds to a ^{29}Si atom in one of the two equivalent sites. Furthermore, on the low-field side of the lowest Zeeman line, we see at higher gains a line whose magnetic field position and intensity is consistent with that expected for ^{29}Si atoms in both of these two equivalent sites.¹⁷ At this point in our EPR studies we have been unable to extract the crucial information (symmetry of the interaction, relative intensity, and anisotropy) buried in the β ^{29}Si hyperfine lines. Consequently, the β ^{29}Si hyperfine interactions will be dropped from further consideration in this paper. A careful search for additional hyperfine lines within 300 Oe of the Zeeman lines was also made, but none was found. We were particularly concerned about finding either a ^{29}Si or ^{13}C hyperfine line arising from a single atom. We also observed the Si-B3 spectrum in our 226 samples which were enriched with ^{13}C ($I = \frac{1}{2}$) to 60.1%; this spectrum is illustrated in Fig. 4. It is important to note that there is no hint of any structure in the Zeeman lines which can be associated with ^{10}B , ^{13}C , or any other group III or V impurity or any splittings which might suggest a distortion in the D_{2d} symmetry of this defect.

The angular dependence in the Si-B3 Zeeman and α ^{29}Si hyperfine lines is plotted in Fig. 5. The degeneracy in the angular dependence of the Si-B3 spectrum indicates that this defect has D_{2d} symmetry.^{18,19} Patterns such as this one are rare and

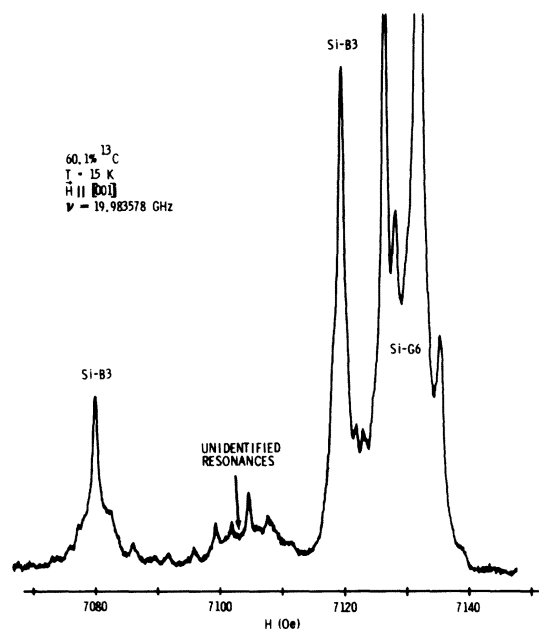


FIG. 4. Si-B3 EPR spectrum. This spectrum was observed in a sample (226) of vacuum-float-zone silicon doped with 10^{15} boron/cm³ and 10^{17} carbon/cm³. The carbon was enriched with ¹³C to 60.1%. This sample was irradiated with 1.20×10^{15} n/cm² and then annealed at 300 °C for 20 min.

indicative of simple defects. So far, such patterns have been observed in connection with the Jahn-Teller distorted positive vacancy (Si-G1),⁶ the spin-1 Si-A5 center,³ and the Si-G25 center.⁵ In the case of the Si-G25 center, Watkins believes that this defect, which is produced following a low-temperature (4.2 K) irradiation with 46 MeV electrons, may possibly be associated with an interstitial.⁵ The apparent simplicity of the Si-B3 center makes it of considerable interest.

The Zeeman and ²⁹Si hyperfine interactions can be represented in terms of a spin Hamiltonian²⁰ of the form

$$\mathcal{H} = \mu_B \vec{H} \cdot \vec{g} \cdot \vec{S} + \sum_k \vec{S} \cdot \vec{A}_k \cdot \vec{I}_k. \quad (1)$$

Since this is an $S = \frac{1}{2}$ center, and the hyperfine interactions are small, the nuclear Zeeman interaction has negligible effect on the observed hyperfine spectra and is therefore omitted from Eq. (1). The numerical values for the \vec{g} and \vec{A} dyadics which characterize the Si-B3 Zeeman and the α ²⁹Si hyperfine interactions are tabulated in Table I.

D. Stress effects

Most defects have a high-temperature stress response which corresponds to an atomic re-

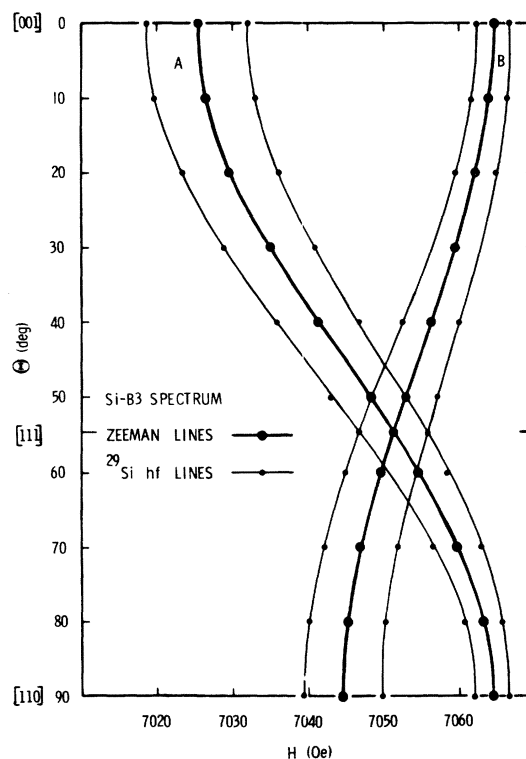


FIG. 5. Plot of the angular dependence in the Si-B3 EPR Zeeman and α ²⁹Si hyperfine spectra. The dots correspond to the experimental data, and the solid lines correspond to the calculated angular dependence using the \vec{g} and \vec{A} dyadics tabulated in Table I.

orientation. If the defect has undergone a Jahn-Teller distortion, then the defect exhibits low-temperature stress effects. The divacancy¹⁴ and carbon interstitialcy,¹⁰ for example, both exhibit these two kinds of reorientation. Stress effects usually give us some additional understanding of the kinetics and structure of a defect.

The Si-B3 center exhibits no low-temperature stress response. In particular, a stress of 1780 kg/cm² was applied uniaxially along the $[\bar{1}10]$ direction of our silicon sample at 310 K (37 °C). While under stress the sample was slowly cooled (≈ 2 K/min) to 20 K, and the stress was then released. The relative intensity of the two Zeeman

TABLE I. Tabulation of the \vec{g} and $\alpha\vec{A}$ dyadics as determined from the Si-B3 spectrum at 20 and 50 K using a microwave frequency of ≈ 20 GHz. The axis of axial symmetry corresponds to a $\langle 001 \rangle$.

\vec{g} dyadic (Ref. 1)		$\alpha\vec{A}$ dyadic (10^{-4} cm ⁻¹)	
± 0.0002		± 0.2	
g_{\parallel}	g_{\perp}	A_{\parallel}	A_{\perp}
2.0166	2.0054	12.8	4.2

lines remained unchanged. This result indicates that the Si-B3 center is not a pointlike defect which has undergone a Jahn-Teller distortion from T_d to D_{2d} symmetry. These results indicate that the Si-B3 center has *inherent* D_{2d} symmetry. Consequently, the structure of the Si-B3 center must correspond to an extended type of defect rather than a pointlike defect. If this is the case, then one would expect the Si-B3 center to exhibit a high-temperature stress response indicative of an atomic reorientation.

By heating a sample containing Si-B3 centers up to 460 °C without stress, a preferential stress-induced alignment can be achieved by cooling the sample to < 350 °C under stress. With a uniaxial stress of 1835 kg/cm² applied along the $[\bar{1}10]$, the ratio $I_A/(I_A+I_B)$ (I_A and I_B are the intensity of the respective lines in Fig. 5) for \bar{H} along the $[001]$ changes from 0.26 (random alignment¹⁶) to 0.41. The recovery from this stress-induced alignment indicates that the Si-B3 center does begin to undergo thermally-activated atomic reorientation for $T \geq 400$ °C. Either the defect is rotating about its center from one equivalent position to another, or it is beginning to tumble through the lattice. The relationship between time τ and temperature T for the thermally-activated reorientation of a defect is usually given^{10,14} by the expression

$$\tau = \tau_0 e^{E/kT}, \quad (2)$$

where E is the activation energy for reorientation. Although we have not yet determined τ_0 from our experimental data, the value for τ_0 for most defects corresponds reasonably well to the theoretical expression h/kT .^{21,22} Since the value of E is rather insensitive to the value of τ_0 , we estimate from our measurements that the activation energy for the atomic reorientation for the Si-B3 center is ≈ 2.3 eV.

Since the Si-B3 center is a secondary defect which forms between ≈ 50 and 175 °C, it is also possible to induce a preferential alignment with stress applied during the formation of the Si-B3 centers. In this procedure a uniaxial stress of 2000 kg/cm² was applied along the $[\bar{1}10]$ direction at room temperature to a sample which had been neutron irradiated but not previously annealed; under these conditions no Si-B3 centers are believed to be initially present in the sample. With the sample under stress, the temperature was subsequently raised to 275 °C and held there for 20 min. Under these conditions the energy of the various immediate configurations of the defect during formation are slightly altered due to strain in the lattice. Consequently, a preferential alignment of the Si-B3 centers with respect to the strain field can be achieved. Once the defect is

formed there is not sufficient thermal energy available at these lower temperatures to excite the defect to another orientation. In order to demonstrate this fact, the stress on our sample was removed at 275 °C and the sample was then heated to 350 °C for 20 min so as to minimize the concentration of other defects and allow the Fermi level to drop to a position nearer the valence band where the Si-B3 centers are paramagnetic due to the loss of an electron. After 20 min at 350 °C the sample was cooled without stress back to room temperature. Under these conditions the number of Si-B3 centers aligned perpendicular to the direction of applied stress is enhanced 20%. We have also observed that this polarization is proportional to the applied stress. Consistent with this interpretation is the following observation. If a neutron-irradiated sample is annealed without stress so that all of the Si-B3 centers which can form are formed, then we observe that it is impossible to quench in a defect alignment by cooling the sample under stress from 350 to ≈ 0 °C. Once a preferential alignment has been achieved by this method, the Si-B3 center begins to undergo thermally activated atomic reorientation at ≈ 400 °C.

From these stress measurements at least six conclusions regarding the Si-B3 center are evident: (i) The Si-B3 center is not Jahn-Teller distorted, which means that it has D_{2d} symmetry by virtue of its molecular structure. (ii) The Si-B3 center is a secondary defect which begins to form somewhere between 50 and 175 °C. (iii) The Si-B3 center exists in at least two charge states with $S=0$ and $S=\frac{1}{2}$. (iv) The Si-B3 center can be aligned under $\langle 110 \rangle$ uniaxially stress during and after formation. (v) Under stress the axis of axial symmetry tends to be aligned perpendicular to the direction of the applied stress. (vi) The Si-B3 center begins to undergo thermally-activated atomic reorientation at ≈ 400 °C with an activation energy of ≈ 2.3 eV.

III. ANALYSIS AND INTERPRETATION

A. Structure of the Si-B3 center

The main features in the Si-B3 center which we are able to see with EPR are illustrated in Fig. 6. Our EPR measurements indicate that this defect has D_{2d} symmetry and is centered on either a lattice site or a tetrahedral interstitial site. This T_d site, which is the center of the defect, appears to be vacant although a silicon atom could possibly occupy this site; this site is not occupied by an impurity atom (Sec. III C). Equidistant from this T_d site along the $\langle 001 \rangle$ direction of axial symmetry are located silicon atoms $Si_{(1)}$ and $Si_{(2)}$.

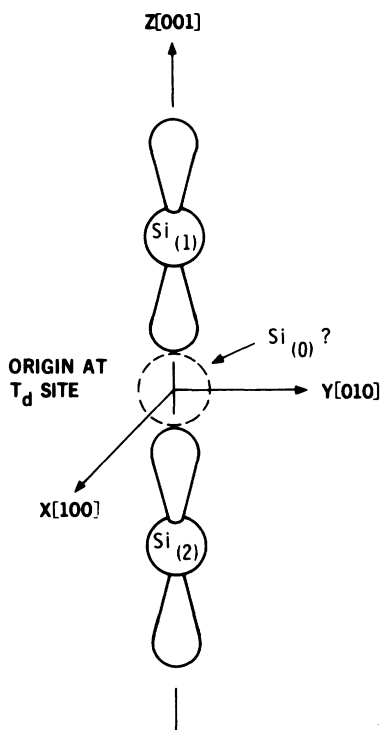


FIG. 6. Basic structure of the Si-B3 center. Silicon atoms $Si_{(1)}$ and $Si_{(2)}$ give rise to the α ^{29}Si hyperfine lines. Whether or not a silicon atom $Si_{(0)}$ resides at the T_d site in the Si-B3 center has not yet been established.

From this basic picture we have developed several models of the Si-B3 center which are illustrated in Fig. 7. These models are characterized by a pair of silicon interstitial atoms, labeled

I_1 and I_2 in Fig. 7, which account for the basic symmetry of the defect. Since this defect is observed with a spin of $\frac{1}{2}$ in p -type material, the Si-B3 center would correspond to the positive charge state of the models in Fig. 7. We will now examine in closer detail those aspects of our data which bear on the various facets in the molecular and electronic structure of these models.

B. Symmetry considerations

One of the most striking features associated with the Si-B3 spectrum is its angular dependence which is indicative of a defect having D_{2d} symmetry.^{18,19} The large number of covering operations in the point group D_{2d} under which the Si-B3 center must be invariant considerably restricts the number of possible geometrical configurations.

The basic rules for deriving acceptable geometrical configurations are summarized as follows. If a point (a, b, c) corresponding to E in Fig. 8 exists, then there are up to seven other sites which are related to the first by the respective covering operations of the point group D_{2d} (class 5). With the aid of Fig. 8 one can see that for certain relationships among a , b , and c , the position of the points are degenerate to various degrees.

Class 1: $a = b = c = 0$. In this case only one site exists. In the diamond lattice this T_d site corresponds to either a lattice or tetrahedral interstitial site since D_{2d} is a subgroup of T_d .

Class 2: $a = b = 0, c \neq 0$. Two nondegenerate sites exist at $(0, 0, \pm c)$. In the diamond lattice these sites are located equidistant from a T_d site

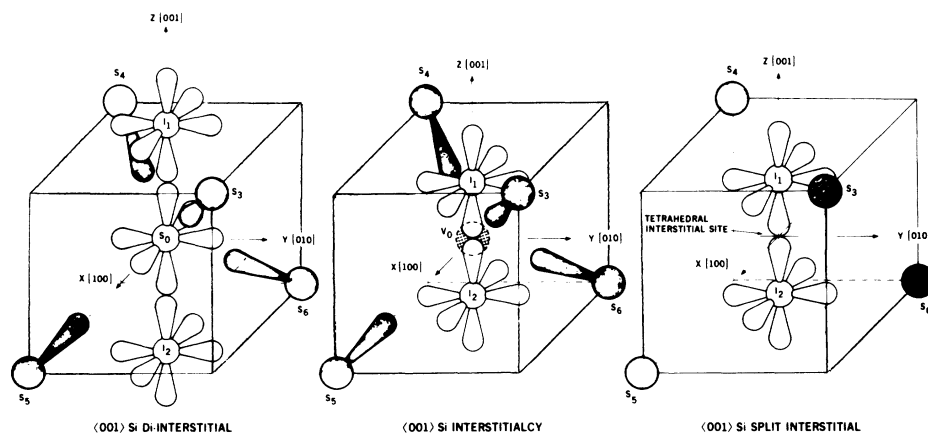


FIG. 7. Models for the Si-B3 center. The shaded atoms correspond to host-lattice atoms. I_1 and I_2 correspond to silicon interstitial atoms. In the $\langle 001 \rangle$ Si di-interstitial S_0 corresponds to a Si atom in a lattice site. In the $\langle 001 \rangle$ Si interstitialcy V_0 corresponds to a silicon vacancy. The $\langle 001 \rangle$ split interstitial is centered on the tetrahedral interstitial site. These three models have inherent D_{2d} symmetry. Although the terminology for naming interstitial complexes has not been standardized, we feel this nomenclature comes the closest to describing the basic structures illustrated here.

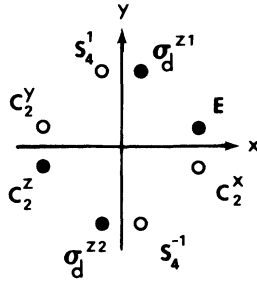


FIG. 8. This array of points represents the most general configuration of points that can have D_{2d} symmetry. The open circles correspond to points with $z = +c$ whereas the solid circles correspond to points with $z = -c$. Each point is identified by a symbol (E , σ_d^{z1} , S_4^1 , etc.) which identifies the particular cover operation in the point group D_{2d} which transforms the point E to that respective point.

on the $[001]$ or z axis.

Class 3: $a = b \neq 0$. Four nondegenerate sites exist at (a, a, c) , $(-a, -a, c)$, $(a, -a, -c)$, and $(-a, a, -c)$. In the diamond lattice these points lie in (110) and $(\bar{1}\bar{1}0)$ planes which contain the $[001]$ direction (z axis).

Class 4: $b = c = 0$, $a = \xi \neq 0$; $a = c = 0$, $b = \xi \neq 0$. Four nondegenerate sites exist at $(\pm \xi, 0, 0)$, $(0, \pm \xi, 0)$. In the diamond lattice these points are located on the $[100]$ and $[010]$ directions; that is, the x and y axes, respectively.

Earlier we indicated that the α ^{29}Si hyperfine interaction arose from two equivalent silicon atoms. According to the rules just summarized, these two silicon atoms can only be located equidistant from a T_d site on a $\langle 001 \rangle$ axis about which the defect has axial symmetry.

C. Role of impurities

The fact that the Si-B3 spectrum can be observed after neutron irradiation and subsequent annealing in boron-doped Lopex silicon but not in aluminum-doped Lopex silicon (Sec. IIA) suggests that either boron plays a unique role in the production of Si-B3 centers or that it is incorporated in the structure of the Si-B3 center. It has been observed that some silicon contains carbon as an impurity.¹⁰ Consequently, whether boron or carbon is incorporated in the structure of the Si-B3 center is of basic concern; we have already established that oxygen is not part of this defect (Sec. IIA). From an analysis of the Si-B3 spectrum we will try to establish the role of impurities in the structure of the Si-B3 center.

According to group theory the wave function for the paramagnetic electron, which is in an orbital singlet, transforms as either Γ_1 or Γ_4 . Molecular orbitals which transform as Γ_1 and Γ_4 are

$$\begin{aligned} \psi(\Gamma_1) = & \eta_{1,0} \psi_{0,s} + \eta_{1,1} (\psi_{1,s} + \psi_{2,s}) \\ & + \eta_{1,2} (\psi_{1,p_z} - \psi_{2,p_z}) + \dots \end{aligned} \quad (3)$$

and

$$\begin{aligned} \psi(\Gamma_4) = & \eta_{4,0} \psi_{0,p_z} + \eta_{4,1} (\psi_{1,s} - \psi_{2,s}) \\ & + \eta_{4,2} (\psi_{1,p_z} + \psi_{2,p_z}) + \dots \end{aligned} \quad (4)$$

In this notation $\eta_{k,l}$ represents the l th coefficient belonging to representation Γ_k ; $\psi_{n,\text{orbital}}$ denotes an atomic orbital centered on atom n in Fig. 7.

If the paramagnetic electron is in a Γ_1 state, then according to group theory every atom in the defect can have an admixture of $\psi_{i,s}$. [For the sake of brevity Eqs. (3) and (4) show only the linear combination of atomic orbitals on sites 0, 1, and 2 in Fig. 7.] Consequently, the contact part of the hyperfine interaction, which is proportional to $|\psi_{i,s}(0)|^2$, gives rise to $2I + 1$ hyperfine lines whose relative intensity is proportional to the abundance of that isotope *and* the number of equivalent sites. Although the envelope of $\psi_{i,s}(\vec{r})$ decreases roughly exponentially with increasing r , one should be able to see resolved or partially resolved hyperfine structure arising from ^{10}B ($I = 3$ and enriched to 95%) or ^{13}C ($I = \frac{1}{2}$ and enriched to 60.1%) within at least the first two or three neighbor shells. No hyperfine structure due to ^{10}B or ^{13}C , or for that matter any other group III, IV, or V impurity, is evident in the Si-B3 spectrum illustrated in Figs. 3 and 4. Furthermore, there is no evidence which suggests that the symmetry of this defect is perturbed by a neighboring impurity atom. In this respect Daly¹ suggested that the Si-B3 might be a vacancy associated with some other defect, like an impurity interstitial located in a $[001]$ direction. This configuration, which would have C_{2v} symmetry, is inconsistent with the D_{2d} symmetry of the defect; in fact, a prototype of Daly's model is the Si-G4 center which Watkins⁵ more recently has identified as a vacancy paired with oxygen in a $\langle 001 \rangle$ direction and which has C_{2v} symmetry. Consequently, for the case in which the paramagnetic electron is in a Γ_1 state, there is no evidence for the existence of impurities in the Si-B3 center.

If the paramagnetic electron is in a Γ_4 state, then the arguments in the previous paragraph apply, but with the following exception. No s -state contributions are allowed by symmetry at the T_d site at the center of the defect and those sites belonging to symmetry class 4 which exist at $(\pm \xi, 0, 0)$ and $(0, \pm \xi, 0)$ (Sec. IIIB). Ideally, this means that the contact part of the hyperfine interaction is zero; however, the dipolar part of the hyperfine interaction should produce splittings in the Zeeman lines that range from 0 to $\approx \mu_n \eta_{4,i}^2 \langle r^{-3} \rangle_p$ depending upon the direction of the applied magnetic field.

Given that $\langle r^{-3} \rangle_{2p} = 15.48 \times 10^{24} \text{ cm}^{-3}$ (Ref. 10), and $\mu_n = 0.7022 \mu_N$ for ^{13}C , or that $\langle r^{-3} \rangle_{2p} = 5.42 \times 10^{24} \text{ cm}^{-3}$ (Ref. 22), and $\mu_n = 1.8005 \mu_N$ for ^{10}B , where μ_N is the nuclear magneton, $\mu_n \eta_{4,i}^2 \langle r^{-3} \rangle_{2p}$ turns out to be $\approx 10 \text{ Oe}$ for $\eta_{4,i}^2 = 0.20$. If $\eta_{4,i}^2$ is less than 0.02, then it becomes difficult if not impossible to detect the presence of impurities in the class 1 and class 4 sites. For a ^{13}C or ^{10}B atom located at the T_d site, one might expect $\eta_{4,0}^2$ to be typically ≈ 0.20 ; therefore, it is very unlikely that either a ^{10}B or ^{13}C atom is located at the T_d site. This argument is exemplified in the case of the Si-G12 center. Recently, it has been established that the Si-G12 center corresponds to a carbon interstitial located on a $\langle 001 \rangle$ axis having C_{2v} symmetry.^{23,24} In this case the paramagnetic wave function transforms as Γ_4 , and the carbon atom is situated at a nodal point in the wave function; therefore, s -state orbitals on the carbon atom are forbidden. Nevertheless, the splittings in the ^{13}C hyperfine lines range from 6 to 52 Oe and $\eta_{\text{carbon}}^2 = 0.33$. In this case the hyperfine spectrum of this atom is readily observable. For these reasons we believe that if the T_d site in the Si-B3 center were occupied by a carbon or boron atom, its hyperfine spectrum would be observable. However, it is rather difficult to say whether a quadrupolar arrangement of ^{10}B or ^{13}C atoms having class-4 symmetry could be detected because of the uncertainty in the value expected for $\eta_{4,i}^2$ (clearly, $\eta_{4,i}^2$ would be a function of ξ). At this point there is no evidence for the existence of impurities in the Si-B3 center.

D. Nature of the ^{29}Si hyperfine interactions

There is no evidence of a ^{29}Si hyperfine spectrum arising from a single silicon atom located at the T_d site. If it could be established that the paramagnetic electron was in a Γ_1 state, then this observation would mean that the T_d site is vacant. However, if the paramagnetic electron is in a Γ_4 state, then two alternatives arise. Either the T_d site is vacant, or it is occupied by a silicon atom but hidden from observation because $\eta_{4,0}^2$ in Eq. (4) is too small. In order to detect this hyperfine interaction, it would have to have an anisotropy of at least 6 Oe (because ^{29}Si is only 4.7% abundant) which corresponds to $\eta_{4,0}^2 \geq 0.13$ assuming no s -state contributions. Even if we expect $\eta_{4,0}^2$ to be 0.2, the discrimination between these two alternatives is rather marginal; whether the T_d site is vacant or occupied with a silicon atom is uncertain at this time.

Vacancy-type defects having D_{2d} symmetry can be modeled, but their properties appear to be inconsistent with the nature of the Si-B3 center. The Si-B3 center cannot be either an isolated

vacancy or an isolated pentavacancy consisting of a vacancy at the T_d site surrounded by four nearest-neighbor vacancies at $\langle 111 \rangle$ sites belonging to symmetry class 3. Both the vacancy, which has been previously identified and associated with the Si-G1 spectrum,⁶ and this pentavacancy would exhibit Jahn-Teller effects in the paramagnetic charge state. The Si-B3 center is not Jahn-Teller distorted (Sec. IID); therefore, these models are unacceptable. Although other simple configurations such as a divacancy with vacancies at class-2 symmetry sites or a tetravacancy with vacancies at class-4 symmetry sites have inherent D_{2d} symmetry, the vacancies in these defects are interspersed among the host-lattice atoms. Interspersed vacancy configurations are inconsistent with previous EPR studies which indicate that vacancies tend to cluster into nearest-neighbor sites.^{14,25-27} It is also important to note that in all of the known vacancy (Si-G1,⁶ Si-G2²), multiple vacancy (Si-G6,¹⁴ Si-G7,¹⁴ Si-P1^{2,26,28}) and vacancy-impurity (Si-G3,^{2,5} Si-G4,^{2,5} Si-G8,²⁹ Si-G23,³⁰ Si-G24,³⁰ and Si-B1³¹) centers having $S = \frac{1}{2}$, at least 55% of the resonant wave function is localized on $\langle 111 \rangle$ broken bonds. (We applied this rule to the recently discovered Si-A4 center³ which Lee and Corbett²⁷ indicate is a $\{110\}$ planar 3 or 5 vacancy center. They indicate a ^{29}Si hyperfine interaction with only one $\langle 111 \rangle$ broken bond on which only 33.6% of the wave function is localized. However, in this case we argue that the symmetry of the Si-A4 \bar{g} dyadic indicates that this defect has C_{2v} symmetry; therefore, the ^{29}Si hyperfine interaction on $\langle 111 \rangle$ bonds has to come in pairs in which case the total localization on $\langle 111 \rangle$ dangling bonds would be at least 67%.) The ^{29}Si hyperfine structure associated with the Si-B3 center in no way reflects this degree of localization on $\langle 111 \rangle$ dangling bonds. For these reasons the Si-B3 center is not believed to be a vacancy-type defect.

The antibonding nature of the defect wave functions suggests that the Si-B3 center is an interstitial type of defect. An analysis, like that done previously on other defects,^{29,31} of the α ^{29}Si hyperfine interaction indicates that only 18% of the paramagnetic wave function is localized on silicon atoms $\text{Si}_{(1)}$ and $\text{Si}_{(2)}$ in Fig. 6. Furthermore, the analysis yields $\eta_{k,1}^2 = 0.0051$ and $\eta_{k,2}^2 = 0.0849$ where $k = 1$ or 4 in Eqs. (3) or (4). This implies that 94% of the wave function on either $\text{Si}_{(1)}$ or $\text{Si}_{(2)}$ is $3p$ -like and only 6% is $3s$ -like. The lack of even any moderately strong ^{29}Si hyperfine interactions tends to suggest that the paramagnetic electron reflects more of an antibonding or nonbonding type of environment. Consistent with this interpretation is the observation that under high-

temperature stress the z axis of the defect tends to align itself perpendicular to the direction of applied stress (Sec. IID). Such behavior is characteristic of a defect which involves antibonding rather than bonding; that is, the defect chooses to align itself so as to minimize rather than maximize orbital overlap. One might expect interstitial-type defects such as those illustrated in Fig. 7 to exhibit antibonding. The fact that the α ^{29}Si hyperfine interaction is the strongest with silicon atoms $\text{Si}_{(1)}$ and $\text{Si}_{(2)}$ suggests that these atoms characterize the defect. In order for these silicon atoms alone to characterize the symmetry of the defect, they have to be interstitials; they cannot be lattice atoms. If indeed they were lattice atoms, then we would be forced to reconsider either another $\langle 001 \rangle$ self-interstitial configuration, a multiple-vacancy, or an impurity configuration which accounts for the inherent D_{2d} symmetry of this defect.

IV. DISCUSSION

A. Nature of interstitials

There is indirect experimental evidence which suggests that self-interstitials produced in irradiated silicon diffuse through the lattice even at low temperatures (4 K).² In view of the models which we have proposed for the Si-B3 center, it is important to consider the following question: Does the low-temperature diffusion of the self-interstitial involve the migration of a single silicon atom through the interstices of the lattice, or does it involve the diffusion of an interstitial defect but not the atoms comprising the defect by means of an interstitialcy mechanism? For example, in metals, diffuse x-ray scattering measurements indicate that self-interstitials migrate at low temperatures (e.g., 5 K in Au and Pb) by means of an interstitialcy mechanism.³² Recently, work done in collaboration with Watkins^{23,24} indicates that the Si-G12 spectrum arises from a single carbon interstitial atom. This carbon interstitial migrates through the silicon lattice for temperatures $\geq 0^\circ\text{C}$. The high-temperature ($T > 0^\circ\text{C}$) diffusion of carbon, which is isoelectronic with silicon, is in sharp contrast to the low-temperature (4 K) diffusion of silicon interstitials. This observation tends to support the idea that the low-temperature migration of silicon interstitials is by means of an interstitialcy mechanism which involves the diffusion of only an interstitial defect but not the specific atoms comprising the defect. If this inference is correct, then the Si-B3 center cannot be a $\langle 001 \rangle$ Si interstitialcy such as illustrated in Fig. 7, because the Si-B3 center remains locked in the lattice for temperatures $\leq 400^\circ\text{C}$.

The fact that the Si-B3 center can be stress aligned during formation suggests that this secondary defect is formed as a result of two defects coming together. Although our experimental measurements do not tell us directly what these defects are, it appears that self-interstitials have been created or released upon annealing and have combined to form the Si-B3 center. Both the $\langle 001 \rangle$ Si di-interstitial and $\langle 001 \rangle$ Si split-interstitial models can be viewed as being composed of two self-interstitials. If this is the case then the $\langle 001 \rangle$ Si split interstitial might look a little more like the complex illustrated in Fig. 9. I_1 and I_2 correspond to the interstitials in the $\langle 001 \rangle$ Si split-interstitial model of Fig. 7. I_{11} and I_{12} may not be completely

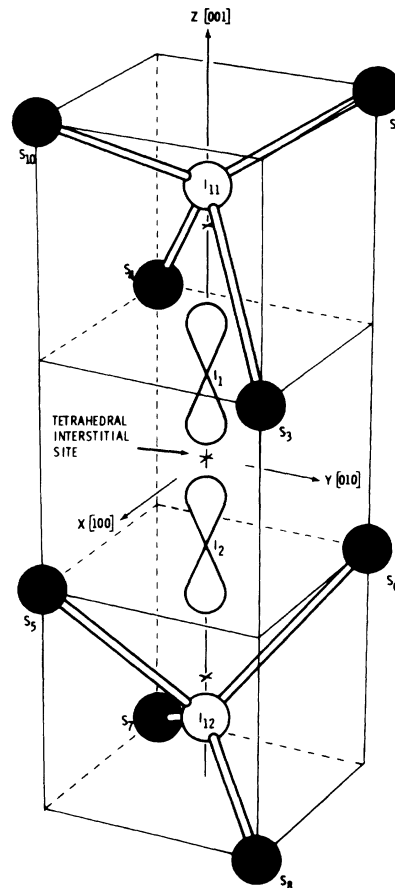


FIG. 9. Extended picture of the $\langle 001 \rangle$ Si split interstitial. The shaded atoms labeled S_3, S_4, \dots, S_{10} correspond to lattice atoms. $I_1, I_{11}, I_2,$ and I_{12} represent silicon interstitials; the α ^{29}Si hyperfine interaction indicates that the paramagnetic wave function on silicon interstitials I_1 and I_2 is 94% p_x -like and only 6% s -like. I_{11} and I_{12} are silicon atoms which are probably displaced outward along the $\langle 001 \rangle$ from their normal lattice sites. In this sense the defect begins to look like a pair of $\langle 001 \rangle$ Si interstitialcies which have formed a stable configuration.

substitutional, but might well be displaced outward along the $\langle 001 \rangle$ axis. In this model I_{11} and I_{12} are spaced equidistant from the tetrahedral interstitial site so that D_{2d} symmetry is preserved. In this extended picture, I_1 and I_{11} as well as I_2 and I_{12} may be viewed as a pair of interstitialcies which have combined to form a stable $\langle 001 \rangle$ Si interstitial complex. Most of the structural detail which we are able to see in this model with EPR is associated with I_1 and I_2 .

B. Relationship to the Si-P6 center

Some years ago Jung and Newell⁷ observed a paramagnetic center (Si-P6) in neutron-irradiated silicon whose principal axes at 300 K were along the $\langle 001 \rangle$ directions. At this temperature the defect appears to have D_2 (not D_{2d}) symmetry.^{18,19} The Si-P6 center can be observed in high-fluence, neutron-irradiated, intrinsic, vacuum-float-zone silicon; and it anneals between 100 and 175 °C.⁷

Recently, Lee and Corbett⁸ have done additional EPR work on this center. They found that as the temperature is lowered to 200 K, its symmetry is reduced to C_2 or C_{1h} . The wave function for the paramagnetic electron transforms as Γ_1 as reflected in the nature of the ²⁹Si hyperfine interactions. This center also exhibits rather unusual motional effects. They have proposed that the motionally averaged Si-P6 center at ≈ 300 K corresponds to a $\langle 001 \rangle$ Si di-interstitial.

Although similar models for the Si-B3 and Si-P6 centers have been proposed, these two defects are definitely not identical. In particular, their symmetries, \bar{g} dyadics, stress response, annealing, and the position of the Fermi level for observation are all different. Clearly, more studies will be required in order to understand the structural differences in these two defects.

C. Relationship to internal-friction measurements

In boron-implanted silicon, Tan, Berry, and Frank⁹ observe four internal-friction peaks. Their peak labeled IV has properties similar to those of the Si-B3 center as observed by EPR. In particular, the annealing of peak IV (Fig. 2 of Ref. 9) is similar to that of the Si-B3 in Fig. 1,³³ or Ref. 1. Also, the symmetry of the Si-B3 center is consistent with the $\langle 001 \rangle$ symmetry of the defect responsible for peak IV. Tan, Berry, and Frank believe that peak IV corresponds to a "neutral $\langle 001 \rangle$ silicon self-interstitial."⁹ Their measurements indicate that their center has an activation energy for atomic reorientation of 0.92 eV whereas the activation energy for atomic reorientation of the Si-B3 center is ≈ 2.3 eV (Sec. IID). The significant difference in the activation

energies for these two defects indicates that they are distinct centers.

V. SUMMARY

The Si-B3 center is a secondary defect which can be formed after neutron irradiation by annealing. In particular, this defect begins to form somewhere between 50 and 175 °C. During formation or after formation it is possible to achieve a preferential alignment in the orientation of this defect; under these conditions the z axis of the defect tends to be aligned perpendicular to the direction of the applied uniaxial stress. The Si-B3 spectrum can be observed in samples which have been annealed anywhere between 175 and 500 °C. At temperatures ≥ 400 °C, the defect undergoes thermally-activated atomic reorientation with an activation energy of ≈ 2.3 eV. So far, the Si-B3 spectrum has only been observed in samples of boron-doped silicon. This spectrum is not observed in samples containing oxygen (e.g., crucible-grown boron-doped silicon) or in aluminum-doped Lopex silicon. This peculiarity suggests that either boron plays a unique role in the production of the Si-B3 center or that it is incorporated in the molecular structure of the defect. Our studies indicate that this latter alternative is unlikely. The Si-B3 center has at least two charge states: the diamagnetic neutral charge state and the paramagnetic positive charge state. It is believed that boron acts as an acceptor for the Si-B3 center in the paramagnetic charge state. As long as there is a supply of acceptors (boron), the number of Si-B3 centers observed after annealing is proportional to the neutron fluence and corresponds to ≈ 0.5 Si-B3 centers/neutron.

The angular dependence in the Si-B3 spectrum indicates that this defect has D_{2d} symmetry. The lack of any low-temperature stress response indicates that this defect is not an isolated defect which has undergone a Jahn-Teller distortion from T_d to D_{2d} symmetry. This rules out the possibility that the Si-B3 center is an isolated Si⁺ tetrahedral interstitial or a pentavacancy consisting of a vacancy surrounded by four nearest-neighbor $\langle 111 \rangle$ vacancies, because these centers would exhibit Jahn-Teller effects. The Si-B3 center does exhibit a high-temperature stress response indicative of an atomic reorientation. This means that the Si-B3 center has inherent D_{2d} symmetry by virtue of its molecular structure.

Although the Si-B3 center has been observed only in boron-doped silicon, there is no direct evidence from our EPR studies which indicates that the Si-B3 center contains carbon or boron.

The electronic structure for this defect is such that the paramagnetic electron is in either a Γ_1 or Γ_4 state. In the Γ_1 state all symmetry sites in the core of the defect are visible through the hyperfine interaction. In the Γ_4 state all symmetry sites except those belonging to symmetry class 4 are visible. We would be blind to boron or carbon (enriched with ^{13}C) on class-1 or class-4 sites if $\eta_{4,i}^2 \leq 0.02$. Although the value for $\eta_{4,i}^2$ on class-4 sites is uncertain, $\eta_{4,0}^2$ on the T_d site is expected to be ≈ 0.20 and therefore visible.

The lack of any strong localization of the paramagnetic electron on $\langle 111 \rangle$ dangling bonds indicates that this center is not a vacancy type of defect. In fact, the small localization of the wave function on neighboring silicon atoms and the tendency of this defect to align under stress so as to minimize orbital overlap suggest antibonding character in the defect wave functions.

These considerations lead us to believe that the Si-B3 center corresponds to a $\langle 001 \rangle$ silicon interstitial complex. Three specific models for this center were considered. The $\langle 001 \rangle$ Si interstitialcy model was rejected because the interstitialcy configuration is believed to be mobile at low temperatures, whereas the Si-B3 center remains locked in the lattice for temperatures $\approx 400^\circ\text{C}$. Even though we do not see a ^{29}Si hyperfine interaction arising from a silicon atom at the T_d site, the $\langle 001 \rangle$ Si di-interstitial is retained as a possible model for the Si-B3 center because if the paramagnetic electron is in a Γ_4 state this silicon

atom might possibly be hidden from observation. The other model for the Si-B3 center corresponds to a $\langle 001 \rangle$ Si split interstitial which is illustrated in Fig. 9 and is consistent with all aspects of our experimental data. These models are characterized by a dumbbell arrangement of Si interstitials centered on a T_d site and correspond to the simplest molecular configurations which have D_{2d} symmetry. Within the context of these models, one might expect the strongest ^{29}Si hyperfine interaction to be associated with the two $\langle 001 \rangle$ Si interstitials I_1 and I_2 . In this respect, the strongest ^{29}Si hyperfine interaction observed in the Si-B3 center does arise with a pair of silicon atoms on the $\langle 001 \rangle$ axis of the defect.

This is the first of what is contemplated to be two papers on this center. During the course of this work we have observed electron-nuclear double resonances arising from ^{29}Si atoms associated with at least ten shells of silicon atoms. Hopefully, this work will enable us to extend our understanding of the molecular and electronic structure of the Si-B3 center.

ACKNOWLEDGMENTS

The competent technical assistance of Roger Shrouf with various aspects of these measurements is greatly appreciated. It is doubtful that this work would have been accomplished without the resources and responsiveness of the Sandia ACPR group who performed the numerous neutron irradiations needed in this work.

*This work was supported by the United States Energy Research and Development Administration, ERDA.

¹D. F. Daly, *J. Appl. Phys.* **42**, 864 (1971).

²G. D. Watkins, in *Radiation Damage in Semiconductors*, edited by P. Baruch (Dunod, Paris, 1965), p. 97.

³Y. H. Lee, Y. M. Kim, and J. W. Corbett, *Radiat. Eff.* **15**, 77 (1972).

⁴H. Alexander, M. Kenn, B. Nordhofen, E. Weber, and W. Sander, in *Lattice Defects in Semiconductors, 1974*, edited by F. A. Huntley (Institute of Physics, London, 1974), p. 433.

⁵G. D. Watkins, in *Lattice Defects in Semiconductors, 1974*, edited by F. A. Huntley (Institute of Physics, London, 1974), p. 1.

⁶G. D. Watkins, *J. Phys. Soc. Jpn. Suppl.* **18**, 22 (1963).

⁷W. Jung and G. S. Newell, *Phys. Rev.* **132**, 648 (1963).

⁸Y. H. Lee and J. W. Corbett, *Solid State Commun.* **15**, 1781 (1974).

⁹S. I. Tan, B. S. Berry, and W. F. J. Frank, in *Ion Implantation in Semiconductors and Other Materials*, edited by B. L. Crowder (Plenum, New York, 1973), p. 19.

¹⁰K. L. Brower, *Phys. Rev. B* **9**, 2607 (1974).

¹¹H. J. Stein (private communication).

¹²K. L. Brower, *Phys. Rev. B* **5**, 4274 (1972).

¹³K. L. Brower, *Phys. Rev. B* **4**, 1968 (1971).

¹⁴G. D. Watkins and J. W. Corbett, *Phys. Rev.* **138**, A543 (1965).

¹⁵L. L. Bonzon, F. M. Morris, and F. V. Thome, Sandia Laboratories Report No. SLA-73-1017 (unpublished).

¹⁶Ideally, the relative intensity of the two Zeeman lines in Fig. 3 should be 1 to 2; however, we observe that there is a deviation in the relative intensities as a function of magnet angle which appears to be due to anomalous variations in the transition matrix elements. This effect is presently not understood and has been noted previously (Ref. 14).

¹⁷The other ^{29}Si pair hyperfine lines are obscured by weak resonances associated with other unidentified defects.

¹⁸F. K. Kneubühl, *Phys. Kondens. Mater.* **1**, 410 (1963); **4**, 50 (1965).

¹⁹J. A. Weil, T. Buch, and J. E. Clapp, *Adv. Mag. Reson.* **6**, 183 (1973).

²⁰B. Bleaney and K. W. H. Stevens, *Rep. Prog. Phys.* **18**, 108 (1953).

²¹J. W. Corbett, in *Radiation Effects in Semiconductors*, edited by F. Seitz and D. Turnbull (Academic, New York, 1966), Suppl. 7, p. 39.

²²G. D. Watkins, *Phys. Rev. B* **12**, 5824 (1975).

- ²³K. L. Brower, *Bull. Am. Phys. Soc.* 21, 364 (1976).
- ²⁴G. D. Watkins and K. L. Brower, *Phys. Rev. Lett.* 36, 1329 (1976).
- ²⁵K. L. Brower, *Radiat. Eff.* 8, 213 (1971).
- ²⁶Y. H. Lee and J. W. Corbett, *Phys. Rev. B* 8, 2810 (1973).
- ²⁷Y. H. Lee and J. W. Corbett, *Phys. Rev. B* 9, 4351 (1974).
- ²⁸M. Nisenoff and H. Y. Fan, *Phys. Rev.* 128, 1605 (1962).
- ²⁹G. D. Watkins and J. W. Corbett, *Phys. Rev.* 134, A1359 (1964).
- ³⁰E. L. Elkin and G. D. Watkins, *Phys. Rev.* 174, 881 (1968).
- ³¹G. D. Watkins and J. W. Corbett, *Phys. Rev.* 121, 1001 (1961).
- ³²W. Schilling, P. Ehrhart, and K. Sonnenberg, in *Fundamental Aspects of Radiation Damage in Metals*, edited by M. T. Robinson and F. W. Young, Jr. (ERDA, Oak Ridge, 1976), p. 470.
- ³³It is interesting to note that since the Si-B3 center does not move until the temperature exceeds $\approx 400^\circ\text{C}$, the gradual decrease in the number of Si-B3 centers between at least 300 and 400 $^\circ\text{C}$ as illustrated in Fig. 1 may be due to annihilation or modification by other mobile defects. If this is the case, then we would expect the number of Si-B3 centers to decrease faster in regions where the lattice damage is denser.